November 2007

Optical Bandgap and Photoconductance of Electrospun Tin Oxide Nanofibers

Yu Wang
University of Puerto Rico

Idalia Ramos
University of Puerto Rico

Jorge J. Santiago-Aviles
University of Pennsylvania, santiago@seas.upenn.edu

Optical Bandgap and Photoconductance of Electrospun Tin Oxide Nanofibers

Abstract
Optical and photoconductive properties of transparent SnO_2 nanofibers, made from $C_{22}H_{44}O_4Sn$ via electrospinning and metallorganic decomposition, were investigated using Fourier transform infrared and ultraviolet (UV)/visible spectrometry and the two-probe method. Their optical bandgap was determined from their UV absorption edge to be 3.95–4.08 eV. Their conductance responds strongly to UV light for a wavelength of 254 nm: in air its steady-state on-to-off ratios are 1.31–1.56 (rise) and 1.25–1.33 (fall); its 90% rise and fall times are 76–96 and 71–111 s, respectively. In a vacuum of about 10^{-4} torr, its on-to-off ratios are higher than 35.6 (rise) and 3.4 (fall), respectively, and its 90% rise and fall times are longer than 3×10^4 s.

Keywords
fibres, fourier transform spectra, infrared spectra, nanostructured materials, nanotechnology, nanostructurred materials, optical constants, photoconductivity, pyrolysis, semiconductor growth, semiconductor materials, tin compounds, ultraviolet spectra, visible spectra

Optical bandgap and photoconductance of electrospun tin oxide nanofibers

Yu Wang
Department of Physics and Electronics, University of Puerto Rico at Humacao, Humacao, Puerto Rico 00791 and Department of Electrical and Systems Engineering, University of Pennsylvania, Philadelphia, Pennsylvania 19104, USA

Idalia Ramos
Department of Physics and Electronics, University of Puerto Rico at Humacao, Humacao, Puerto Rico 00791

Jorge J. Santiago-Avilés[a)]
Department of Electrical and Systems Engineering, University of Pennsylvania, Philadelphia, Pennsylvania 19104, USA

(Received 31 May 2007; accepted 21 August 2007; published online 12 November 2007)

Optical and photoconductive properties of transparent SnO_2 nanofibers, made from $C_{22}H_{44}O_4Sn$ via electrospinning and metallorganic decomposition, were investigated using Fourier transform infrared and ultraviolet (UV)/visible spectrometry and the two-probe method. Their optical bandgap was determined from their UV absorption edge to be 3.95–4.08 eV. Their conductance responds strongly to UV light for a wavelength of 254 nm: in air its steady-state on-to-off ratios are 1.31–1.56 (rise) and 1.25–1.33 (fall); its 90% rise and fall times are 76–96 and 71–111 s, respectively. In a vacuum of about 10^{-4} torr, its on-to-off ratios are higher than 35.6 (rise) and 3.4 (fall), respectively, and its 90% rise and fall times are longer than 3×10^4 s. © *2007 American Institute of Physics*. [DOI: 10.1063/1.2800261]

INTRODUCTION

Transparent conductive oxides (TCOs) have received extensive attention because of their important optoelectronic applications such as electrochromic devices, transparent electrodes, and antireflection coatings in solar cells.[1] Tin oxide or stannic oxide (SnO_2) is a typical TCO with a tetragonal rutile structure and a bandgap (E_g) of around 3.6 eV, which makes it transparent to light up to the ultraviolet (UV).[2] It is also chemically inert, mechanically hard, and thermally heat resistant and has seen additional applications as sensors, heat mirrors, and heterogeneous catalysts.[3] Its conductivity can be changed drastically either by extrinsic impurity doping or by intrinsic formation of oxygen vacancies in its lattice, which donate electrons.[2,3] Since film is the preferred morphology for most optoelectronic, sensing, and heat reflecting applications, SnO_2 films have been synthesized by numerous methods,[1–3] such as chemical vapor deposition,[4] sol-gel,[5] spray pyrolysis,[6] and polymeric precursor,[7] and their electrical and optical properties have been well characterized.[1–7] However, for many applications such as the line light source or dielectric waveguide, the fiber morphology is more favorable. Unfortunately, so far only a few ways, such as thermal decomposition,[8] template and oxidization,[9] laser ablation or vapor-liquid-solid growth,[10] vapor deposition,[11,12] and electrospinning,[13–15] have been developed to fabricate SnO_2 nanofibers or ribbons. Their optical and optoelectronic properties have been only barely touched[10–13] even though such property characterization is indispensable for their optoelectronic applications. For example, only Liu *et al.*,[10] Lee *et al.*,[11] and Mathur *et al.*[12] have evaluated the photoconductance of SnO_2 nanowires and only Lee *et al.* have presented their UV photoresponse.[11] To our knowledge, no report has been made neither on the optical bandgap (E_o) of SnO_2 nanowires, an important parameter for their optoelectronic applications in general, nor on the photoconductance of electrospun SnO_2 nanofibers. We have developed two recipes for electrospinning SnO_2 fibers,[14–16] characterized their electrical properties,[17] and applied a single electrospun SnO_2 fiber in gas detection.[18] This letter investigates their optical and photoconductive properties, with its emphasis on the determination of their optical bandgap and evaluation of their conductive response to UV light.

EXPERIMENT

The synthetic procedure and characterization methods for SnO_2 fibers have been reported in details.[15,16] Briefly, precursor fibers and mats were electrospun from a solution of commercial poly(ethylene oxide) (molecular weight of 900 000), chloroform, and dimethyldineodecanoate tin ($C_{22}H_{44}O_4Sn$) using a homemade electrospinning setup[15] onto quartz plates, for subsequent spectral characterization, and (111)-oriented single crystal silicon wafers with their surface thermally oxidized and patterned with gold contacts, for subsequent conductive measurement. The as-deposited precursor fibers and mats were subsequently thermally decomposed in air for 2 h at 100, 200, 300, 400, 500, and 600 °C, respectively. Our previous x-ray diffraction, Raman microspectrometry, and Fourier transform infrared (FTIR) spectrometry characterization indicated that the fibers are rutile-structured SnO_2 after thermal decomposition at and

a)Electronic mail: santiago@seas.upenn.edu

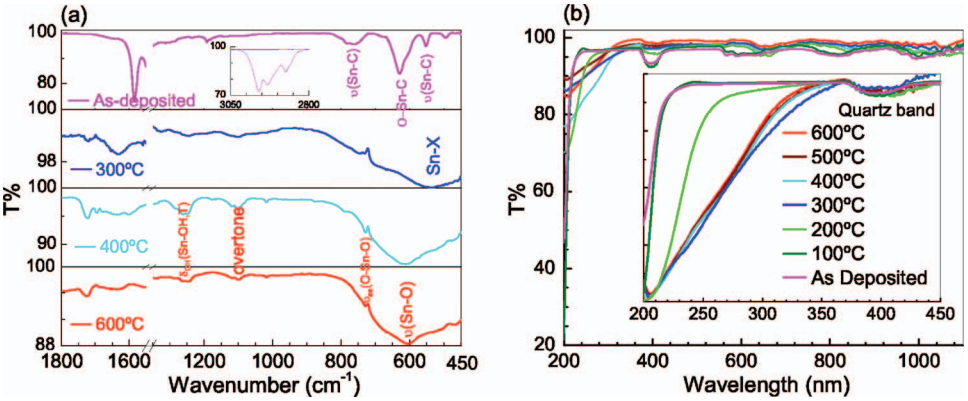

FIG. 1. (Color) (a) FTIR and (b) UV/VIS spectra of as-deposited and thermally decomposed fibers. [The inset in (a) shows the disappearance of the C–H stretching band].

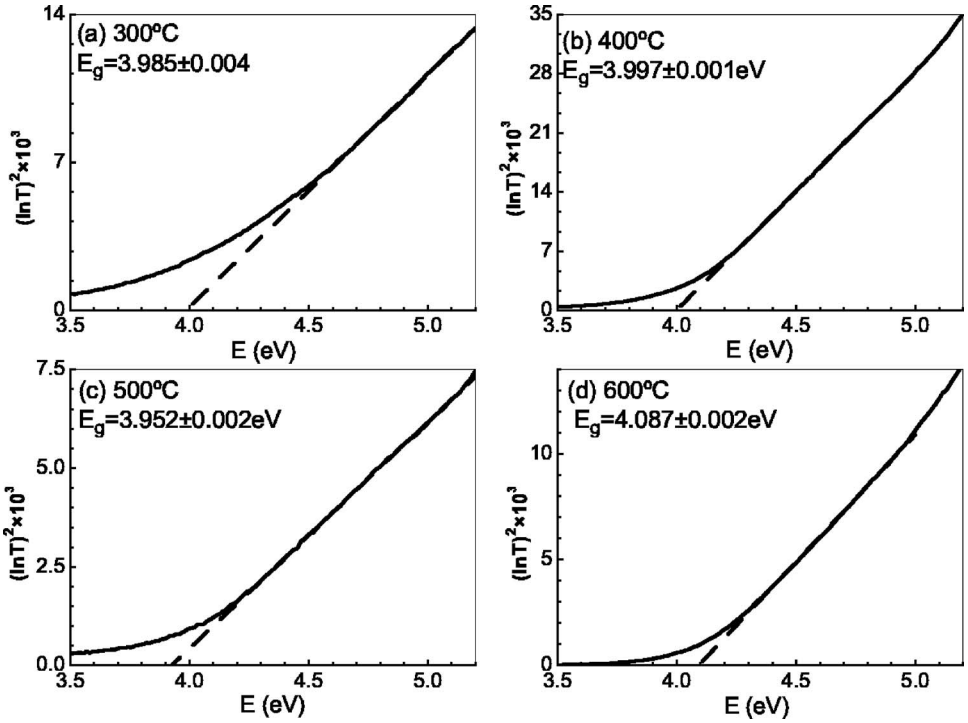

FIG. 2. Determination of optical bandgap (E_o) from the UV absorption edge. (Solid and dashed curves are experimental and linear fitting/extrapolating, respectively.)

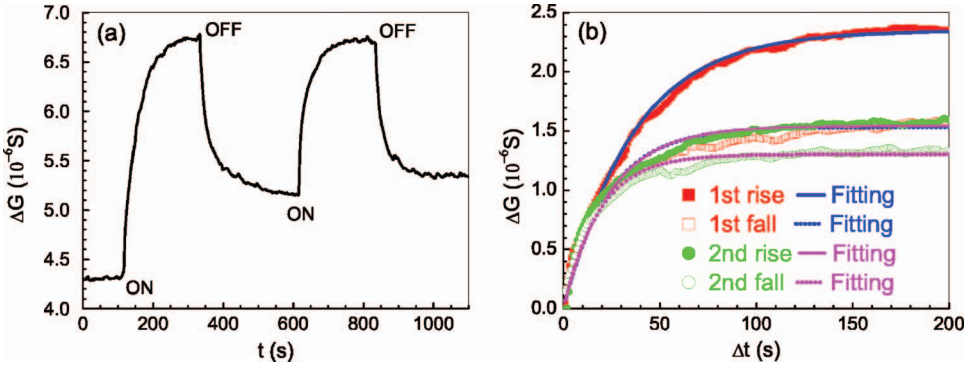

FIG. 3. (Color) Transient UV responses in air: (a) G vs t (time) and (b) ΔG vs Δt.

above 400 °C.[15,16] Optical properties of mats decomposed at different temperatures were measured using a Perkin-Elmer Spectrum One FTIR spectrometer and a Perkin-Elmer Lambda 35 ultraviolet/visible (UV/VIS) spectrometer. Mat samples were directly used for the UV/VIS analysis. For the FTIR analysis, mats were mechanically stripped off their substrate as powder which was sampled using the Nujol-mulling technique.[16] Electrical measurement was conducted on a single fiber decomposed at 600 °C using the two-probe method in air and in a vacuum about 10^{-4} torr. The UV light source is a Minerallight UVGL-25 lamp with its maximum output power density of 460 $\mu W/cm^2$ at the wavelength (λ) of 254 nm.

RESULTS AND DISCUSSIONS

FTIR spectra [Fig. 1(a)] reveal that organic groups in precursor fibers decompose mostly between 200 and 300 °C and the fibers transform into incipient polycrystalline rutile structure at around 400 °C.[16] The synthesized fibers demonstrate a strong absorption band around 600 cm^{-1}, characteristic of the stretching Sn–O vibration of transverse E_u mode in the rutile-structured SnO_2.[19,20] On the other hand, the fibers are transparent from near IR ($\lambda = 1100$ nm) to their UV absorption edge. The edge shifts toward the longer wavelength when the thermal decomposition temperature (TDT) increases from 100 to 300 °C, above which further shift is not evident [Fig. 1(b)].

It is well accepted that the bandgap is direct in the rutile-structured SnO_2.[1–3] During its direct interband transition, the optical absorption coefficient α follows as a function of incident photon energy (E) on the long-wavelength (low E) side,

$$\alpha = [A(E - E_o)]^{1/2}, \tag{1a}$$

or

$$\alpha^2 = A(E - E_o), \tag{1b}$$

where E_o is the optical bandgap and A is a constant.[21] Since α and transmittance (T) are correlated as

$$T = e^{-\alpha L}, \tag{2a}$$

or

$$\alpha = -(\ln T)/L, \tag{2b}$$

where L is the thickness of the sample, we have

TABLE I. Optical bandgap determined from UV absorption edge.

TDT (°C)	300	400	500	600
E_o (eV)[a]	3.985±0.004	3.997±0.001	3.952±0.002	4.087±0.002

[a]The errors given in this report are fitting errors.

$$(\ln T)^2 = AL^2(E - E_o), \tag{3}$$

which predicts a linear relation between $(\ln T)^2$ and E. Such a linear relation is confirmed in the photon energy range of 4.3–5.2 eV (Fig. 2), and its extrapolation to the E-axis gives us E_o values for different TDTs (Table I). Overall, the E_o value increases with heat treatment temperature (HTT) but the variation is very small. The values lie within the reported range of 3.8–4.2 eV for SnO_2 thin film determined in the same way[5–7] and are higher than $E_g \approx 3.6$ eV. The difference may be attributed to the Burnstein-Moss effect[22,23] (due to the filling of the conduction band by free carriers[24]), the two-dimensional quantum confinement (quantum wire) effect caused by the porosity,[25] as well as the defect effect.[5] In literature (Ref. 26, for example), α^i ($i = 1/2, 1$) and $(\alpha E)^j$ ($j = 1/2$, 1, and 2) against E have also been linearly fitted and extrapolated to determine E_o values. Such processing sometimes results in approximately the same E_o values as listed in Table I or values closer to the E_g value. However, they are based on assumptions that cannot be justified for rutile-structured SnO_2 (for example, an indirect bandgap) (Ref. 27) and are not adopted here.

The fiber's conductance (G) is insensitive to visible light, which is consistent with its transparency to visible light [Fig. 1(b)]. However, G is sensitive to UV light of 254 nm wavelength (Figs. 3 and 4). Upon the UV illumination in air, G increases sharply and then asymptotically to its steady value with the on-to-off ratio (ξ) of 1.58 (first cycle) and 1.31 (second cycle); when the UV light is turned off, G decreases asymptotically to its new steady values with $\xi = 1.33$ (first cycle) and 1.25 (second cycle). The 90% rise and fall times (t_r and t_f) of the conductance are 111 and 96 s (first cycle) and 76 and 71 s (second cycle), respectively. It is also interesting that G changed by 19.6% after the first UV on-and-off cycle, implying an only partially irreversible change. However, its change is only 3.5% in the second cycle. In fact, the G change follows

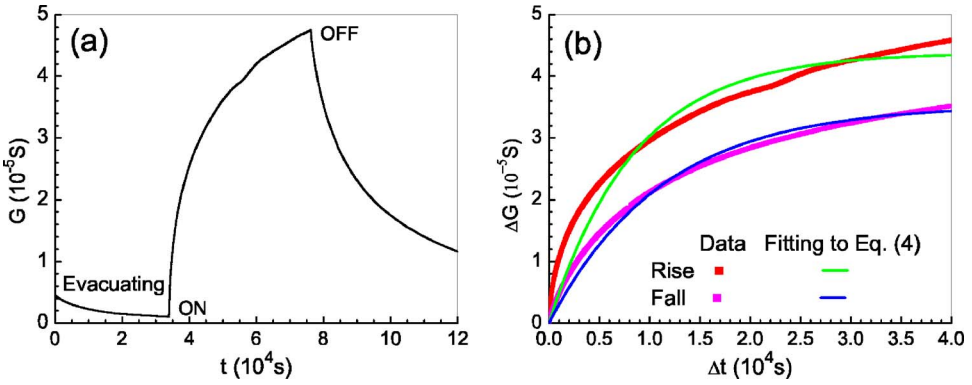

FIG. 4. (Color online) Transient UV responses in vacuum of $\sim 10^{-4}$ torr: (a) G vs time and (b) $\Delta\sigma$ vs Δt.

TABLE II. Main photoresponsive characteristics of the fiber.

Environment	Cycle	ξ	t_r or t_f (s)	ΔG_0 (μS)	τ (s)
In air	First rise	1.56	t_r=96	2.349±0.009	36.1±0.5
	First fall	1.33	t_f=111	1.533±0.006	23.1±0.5
	Second rise	1.31	t_r=76	1.543±0.005	23.7±0.4
	Second fall	1.25	t_f=71	1.304±0.003	18.5±0.3
In vacuum	Rise	>35.6	t_r>30432	4.384±0.002	8522±15
	Fall	>3.40	t_f>30910	3.536±0.001	11227±11

$$\Delta G = \Delta G_0(1 - e^{-\Delta t/\tau}), \tag{4}$$

where Δt is the time measured from the UV-switching moment and ΔG_0 and τ are listed in Table II. While ΔG_0 is proportional to ξ, τ is also a measure of response time, corresponding to ΔG change by 63.8% and less than t_r and t_f (Table II). The wide optical bandgap and high photoconductivity imply promising optoelectronic applications of the nanofibers. It is noteworthy that the photoresponse times and gas-sensing response times[18] are close, both characteristic of the surface adsorption and desorption processes triggered by switching of either analyte or UV light.[11,28,29]

In air, the adsorption of oxygen on the SnO_2 surface can be depicted by the relation,

$$O_2(g) + e^- = O_2^-(ad). \tag{5}$$

It consumes free electrons in SnO_2, bends the conducting band immediately below the adsorbing surface and grain boundaries, and produces a depletion layer that resists electron transport. Since the incident UV light has a photon energy (4.89 eV) higher than E_o, it generates nonequilibrium electron-hole pairs. Some photogenerated holes (h^+) further detach O_2^- from the SnO_2 surface,

$$O_2^-(ad) + h^+ = O_2(g), \tag{6}$$

and reduce the thickness of the depletion region. Both mechanisms contribute to the observed increase of conductance, i.e., photoconductance. When the UV light is off, the reverse processes occur and G decreases.

Dark conductance in vacuum is less than that in air due to the evacuation of the reducing moisture from the chamber. G shows a stronger, though sluggish response to the UV light in vacuum. As soon as the UV light is turned on, G increases monotonously for 44 ks by a factor of 35.56 without stabilization. After the UV light is off, G decreases for 51 ks by a factor of 3.40 without stabilization, either [Fig. 4(a)]. Since G stabilization lasts longer than our measuring system (especially its vacuum pump) can work continuously, t_r and t_f cannot be evaluated as in air. However, they must be longer than the time it takes G to change 90% of the measured maximum ΔG values, 30 432 s (rise) and 30 910 s (fall), which are in turn longer than t_r and t_f in air by two orders of magnitude (Table II). So far as the measured ΔG is concerned, it also roughly follows Eq. (4), and its main characteristics are also listed in Table II. The photoresponse of our electrospun SnO_2 nanowires is similar to those of thermally evaporated SnO_2 nanowires.[11] Since the vacuum was only about 10^{-4} torr, there still were oxygen molecules in the chamber and therefore adsorbed O_2^- species on the SnO_2 surface. The adsorption and desorption processes discussed in the previous paragraph still work, only with a lower partial pressure of oxygen (P_{O_2}), a lower surface concentration of O_2^- ($[O_2^-]$), and accordingly, a thinner depletion layer than in air. The thinner depletion layer can be totally eliminated by the UV illumination and G will be increased more in vacuum than in air. Kinetically, however, the lower P_{O_2} and $[O_2^-]$ values slow down reactions (4) and (5) in vacuum, resulting in longer photoresponse times than in air.

CONCLUSIONS

Optical and photoconductive properties of electrospun tin oxide nanofibers were investigated in UV, VIS, and IR ranges. It was found that the fibers are transparent from 1100 nm to their UV absorption edge. Their optical bandgap lies between 3.95 and 4.08 eV. In air, the conductance of a fiber heat treated at 600 °C responds sensitively to UV light of 254 nm wavelength (4.89 eV photon energy), with its steady on-to-off ratios 1.31–1.56 (rise) and 1.25–1.33 (fall) and its 90% rise and fall times between 76–96 and 71–111 s, respectively. The photoresponse in vacuum is stronger and slower, with the on-to-off ratios higher than 35.6 (rise) and 3.4(fall), respectively, and the 90% rise and fall response times longer than 3×10^4 s.

ACKNOWLEDGMENTS

The authors would like to thank Professor Jack Fischer, with the Laboratory for the Research on the Structure of Matter at the University of Pennsylvania, for his theoretical help. This work was supported by NSF-DMR-0353730 (Penn-UPR Partnership for Research and Education in Materials) and the Nano/Bio Interface Center through the National Science Foundation NSEC DMR-0425780.

[1] K. L. Chopra, S. Major, and D. K. Panda, Thin Solid Films **102**, 1 (1983).
[2] Z. M. Jarzebski and J. P. Marton, J. Electrochem. Soc. **123**, 199C (1976); **123**, 299C (1976); **123**, 333C (1976).
[3] M. Batzill and U. Diebold, Prog. Surf. Sci. **79**, 47 (2005).
[4] D. Davazoglou, Thin Solid Films **302**, 204 (1997).
[5] C. Terrier, J. P. Chatelon, and J. A. Roger, Thin Solid Films **295**, 95 (1997).
[6] S. Shanthi, C. Subramanian, and P. Ramasamy, Cryst. Res. Technol. **34**, 1037 (1999).
[7] T. R. Giraldi, M. T. Escote, A. P. Maciel, E. Longo, E. R. Leite, and J. A. Varela, Thin Solid Films **515**, 2678 (2006).
[8] C. Xu, G. Xu, Y. Liu, X. Zhao, and G. Wang, Scr. Mater. **46**, 789 (2002).
[9] A. Kolmakov, Y. Zhang, G. Cheng, and M. Moskovits, Adv. Mater. (Weinheim, Ger.) **15**, 997 (2003).
[10] Z. Liu, D. Zhang, S. Han, C. Li, T. Tang, W. Jin, X. Liu, B. Lei, and C.

Zhou, Adv. Mater. (Weinheim, Ger.) **15**, 1754 (2003).
[11]J.-S. Lee, S.-K. Sim, B. Min, K. Cho, S. W. Kim, and S. Kim, J. Cryst. Growth **267**, 145 (2004).
[12]S. Mathur, S. Barth, H. Shen, J.-C. Pyun, and U. Werner, Small **1**, 713 (2005).
[13]N. Dharmaraj, C. H. Kim, K. W. Kim, H. Y. Kim, and E. K. Suh, Spectrochim. Acta, Part A **64**, 136 (2006).
[14]Y. Wang, M. Aponte, N. Leon, I. Ramos, R. Furlan, N. Pinto, S. Evoy, and J. J. Santiago-Avilés, J. Am. Ceram. Soc. **88**, 2059 (2005).
[15]Y. Wang, M. Aponte, N. Leon, I. Ramos, R. Furlan, S. Evoy, and J. J. Santiago-Avilés, Semicond. Sci. Technol. **19**, 1057 (2004).
[16]Y. Wang, I. Ramos, and J. Santiago-Avilés, Nanotechnology **18**, 295601 (2007).
[17]Y. Wang, I. Ramos, and J. Santiago-Avilés, IEEE Trans. Nanotechnol. (submitted).
[18]Y. Wang, I. Ramos, and J. Santiago-Avilés, IEEE Sens. J. (in press).
[19]D. Amalric-Popescu and F. Bozon-Verduraz, Catal. Today **70**, 139 (2001).
[20]R. Summitt, J. Appl. Phys. **39**, 3762 (1968).
[21]J. Bardeen, F. J. Blatt and L. H. Hall, in *Photoconductivity Conference, Atlantic City, 1954*, edited by R. G. Breckenridge, B. R. Russell, and E. E. Hahn, (Wiley, New York, 1956).
[22]E. Burstein, Phys. Rev. **93**, 632 (1954).
[23]T. S. Moss, Proc. Phys. Soc. London **67**, 775 (2001).
[24]J. D. Ye, S. L. Gu, S. M. Zhu, S. M. Liu, Y. D. Zhang, R. Zhang, and Y. Shi, Appl. Phys. Lett. **86**, 192111 (2005).
[25]V. Lehmann and U. Gosele, Appl. Phys. Lett. **58**, 856 (1991).
[26]T. D. Senguttuvan and L. K. Malhotra, Thin Solid Films **289**, 22 (1996).
[27]J. I. Pankove, *Optical Processes in Semiconductors* (Dover, New York, 1971), Chap. 3, pp. 22–33.
[28]D. A. Melnick, J. Chem. Phys. **26**, 1136 (1957).
[29]R. Keezer, J. Appl. Phys. **35**, 1866 (1961).